Multiple oscillatory rhythms determine the temporal organization of perception

Luca Ronconi[a,1], Nikolaas N. Oosterhof[a], Claudia Bonmassar[a], and David Melcher[a]

[a]Center for Mind/Brain Sciences, University of Trento, 38068 Rovereto, Italy

Edited by David J. Heeger, New York University, New York, NY, and approved November 7, 2017 (received for review August 17, 2017)

Incoming sensory input is condensed by our perceptual system to optimally represent and store information. In the temporal domain, this process has been described in terms of temporal windows (TWs) of integration/segregation, in which the phase of ongoing neural oscillations determines whether two stimuli are integrated into a single percept or segregated into separate events. However, TWs can vary substantially, raising the question of whether different TWs map onto unique oscillations or, rather, reflect a single, general fluctuation in cortical excitability (e.g., in the alpha band). We used multivariate decoding of electroencephalography (EEG) data to investigate perception of stimuli that either repeated in the same location (two-flash fusion) or moved in space (apparent motion). By manipulating the interstimulus interval (ISI), we created bistable stimuli that caused subjects to perceive either integration (fusion/apparent motion) or segregation (two unrelated flashes). Training a classifier searchlight on the whole channels/frequencies/times space, we found that the perceptual outcome (integration vs. segregation) could be reliably decoded from the phase of prestimulus oscillations in right parieto-occipital channels. The highest decoding accuracy for the two-flash fusion task (ISI = 40 ms) was evident in the phase of alpha oscillations (8–10 Hz), while the highest decoding accuracy for the apparent motion task (ISI = 120 ms) was evident in the phase of theta oscillations (6–7 Hz). These results reveal a precise relationship between specific TW durations and specific oscillations. Such oscillations at different frequencies may provide a hierarchical framework for the temporal organization of perception.

oscillations | vision | alpha | theta | MVPA

Perception has the primary role of reducing the complexity of our environment, since sensory inputs cannot be processed with zero lag in an analog fashion. In the temporal domain, this is demonstrated by many examples whereby stimuli presented at specific temporal delays are sometimes faithfully perceived as separate entities, while they are integrated into a unified or "average" percept in other situations. For example, two flashes separated by a brief temporal delay of about ∼30–40 ms are often perceived as a single flash (1). Similarly, in the perception of apparent motion (2), two stimuli flashed in different spatial locations are often perceived as a single, continuously moving stimulus over a period of hundreds of milliseconds (3). Likewise, in forward- and backward-masking paradigms, a target and mask stimulus may be combined into a single percept, hiding the target, even when separated by around 100 ms (4).

A long-standing hypothesis is that whether two stimuli are integrated or not depends on whether they fall within the same cycle of a neural oscillation (5–8). More recently, the phase of ongoing neural oscillations, especially in the theta and alpha bands (5–7 Hz and 8–12 Hz, respectively), has been found to be related to trial-by-trial fluctuations in threshold-level perception in the visual [theta (9–12) and alpha (9, 10, 13, 14)] and auditory [theta (15) and alpha (16)] domains. However, there is evidence that prestimulus oscillations do not only influence processing of near-threshold stimuli. The oscillatory phase also predicts reaction times [alpha (17, 18) and alpha/lower beta (19)] and is linked to spatial attention [theta (20–22) and beta (23)]. Moreover, the phase of oscillations in the time period before the stimulus onset is correlated to large-scale signatures of stimulus processing, such as event-related potentials (ERPs), BOLD response, and connectivity [theta (12) and alpha (24–26)]. These findings connect to the idea that the phase of neural oscillations reflects the rapid time-scale modulation of cortical excitability (27, reviewed in refs. 28–31). Accordingly, studies in nonhuman primates show that spikes in sensory areas are more likely to occur at a specific phase of the local field potential oscillations relative to the opposite phase (32, 33).

There is some preliminary support for the idea that temporal segregation/integration of visual stimuli depends on oscillatory phase (8, 34–37). However, as mentioned above, there are multiple temporal windows (TWs) in perception, ranging from tens of milliseconds (1) to 80–120 ms (3, 35), to a few hundred milliseconds (38), up to a TW of around 2 s (39–43).

Here, we tested whether the TWs of different length reported in the literature map onto a single oscillatory frequency band, such as the fluctuation in cortical excitability linked to alpha (28–31) or, rather, would be mapped into different, specific oscillatory rhythms. In theory, such a hierarchy of TWs could help to mask the presence of perceptual samples/cycles, which is important, given that the presence of discrete windows in sensory processing does not mean that conscious perception is typically discontinuous (44–46). To accomplish this goal, we measured electroencephalography (EEG) activity while subjects were performing a temporal integration/segregation task involving two different TWs. Then, we applied multivariate decoding analysis to test whether the perceptual outcome of a single trial could be predicted from the phase of the ongoing oscillations and whether

Significance

To reduce the complexity of our sensory environment, the perceptual system discretizes information in different ways. In the time domain, this is evident when stimuli that are presented very close in time are sometimes faithfully perceived as different entities, whereas they are integrated into a single event at other times. Using multivariate decoding of electroencephalography data, we show that integration and segregation of stimuli over different time scales (a few tens vs. a few hundreds of milliseconds) do not rely on a single sampling rhythm; instead, they depend on the phase of prestimulus oscillations at different frequency bands in right posterior-parietal channels. These findings suggest the existence of a specific mapping between oscillations and temporal windows in perception.

Author contributions: L.R. and D.M. designed research; L.R. and C.B. performed research; L.R. and N.N.O. analyzed data; and L.R., N.N.O., and D.M. wrote the paper.

The authors declare no conflict of interest.

This article is a PNAS Direct Submission.

[1]To whom correspondence should be addressed. Email: luca.ronconi@unitn.it.

This article contains supporting information online at www.pnas.org/lookup/suppl/doi:10.1073/pnas.1714522114/-/DCSupplemental.

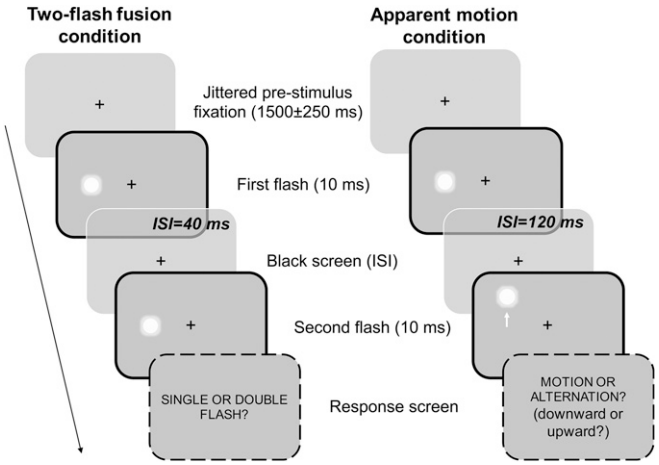

Fig. 1. Schematic representation of the task procedure with the two different types of trial employed. The two types of bistable stimuli used in the present study could appear randomly in the left or right visual hemifield. The stimuli were physically always the same, but their perceptual interpretation varied such that participants perceived one single flash (static or moving) in about half of the trials and they perceived two different flashes (in the same or different positions) in the other half.

the frequency of these oscillations changed as a function of the TW size.

On each trial (Fig. 1), we presented two suprathreshold flashes that could appear randomly in the left or right visual hemifield and either repeated in the same position (two-flash fusion condition) or appeared in a different position (apparent motion condition), with these two conditions randomly intermixed across trials. We manipulated the interstimulus interval (ISI) between the two flashes in a way that induced a bistable perception for both types of visual discrimination, so that subjects integrated (fusion or apparent motion) or segregated (two distinct flashes in the same position or in different positions) the two visual stimuli in about half of the trials. We then used a naive Bayes classifier searchlight on the whole channels/frequencies/times space to decode the perceptual interpretation of this bistable stimulus (segregation vs. integration) from the phase of ongoing oscillations on a trial-by-trial basis, confirming these results also with a more traditional phase-bifurcation analysis (9).

Results

Perceptual Outcome. Perceptual judgments of the stimuli, appearing randomly in the left or right visual hemifield, were almost perfectly bistable in both types of trial (two-flash fusion and apparent motion), which were randomly intermixed during the course of the experiment (*Methods*). Participants (n = 27) perceived two distinct flashes on average on 47.2% (SD = 13%) of trials in the two-flash fusion condition and 49.6% (SD = 14%) of trials in the apparent motion condition. The two trial types did not differ significantly in the rate of segregation/integration trials [$t_{(26)} = -0.7$, $P = 0.49$]. These results suggest that ISI values employed here, which were chosen based on extensive pilot testing, effectively caused the two stimuli to be integrated on about half of the trials.

ERPs of Perceptual Integration vs. Segregation in the Poststimulus Period. First, electrophysiological signatures of integration and segregation of the two flashes in the poststimulus period were assessed by analyzing the mean amplitude of the P1 and N1 ERP components locked to the onset of the first stimulus. A 2 (outcomes: segregation vs. integration) × 2 (hemifields: left vs. right) × 2 [regions of interest (ROIs): left parieto-occipital vs. right parieto-occipital channels] repeated-measure ANOVA on the N1 mean amplitude in the two-flash fusion condition revealed a main effect of ROIs [$F_{(1,26)} = 26.42$, $P < 0.001$] and outcomes [$F_{(1,26)} = 17.15$, $P < 0.001$] and, importantly, an outcomes × ROIs interaction [$F_{(1,26)} = 10.73$, $P = 0.003$]. This two-way interaction, when further explored with post hoc comparisons (two-tailed t tests) revealed a more negative N1 mean amplitude in the segregation trials (i.e., two flashes perceived in the same position) for electrodes that were contralateral to the stimulus presentation [$t_{(26)} = -4.89$, $P < 0.001$] (Fig. 2). For the similar ANOVA performed on the N1 mean amplitude elicited in the apparent motion condition, the main effect of hemifield [$F_{(1,26)} = 28.94$, $P < 0.001$] and the hemifields × ROIs interaction [$F_{(1,26)} = 6.23$, $P = 0.019$] were found to be significant. Importantly, a hemifields × outcomes interaction was also significant [$F_{(1,26)} = 4.83$, $P = 0.037$]. When explored with post hoc tests, this interaction revealed a more negative N1 amplitude for segregation trials (i.e., two flashes perceived in different positions) only for stimuli displayed in the left [$t_{(26)} = -2.61$, $P = 0.015$], but not right [$t_{(26)} = -0.49$, $P = 0.63$], visual hemifield. The same ANOVA on the P1 mean amplitude did not reveal any significant effects.

Decoding Segregation vs. Integration from Single-Trial Phase Information in the Prestimulus Period. The main analysis involved determining whether prestimulus phase information could predict perceptual outcome in the two bistable stimulus conditions. The decoding accuracy for the different perceptual outcomes obtained with the naive Bayes classifier searchlight performed on single-trial phase values is shown in Fig. 3 *A* and *B*. The highest decoding accuracy was found in right posterior parietal channels for both experimental conditions (maximum effects were observed for channels P6, P8, PO8, and O2; Fig. 3 *A* and *B*). Cluster-corrected permutation tests revealed, however, that the time/frequency region in which the maximum decoding accuracy was observed was different between the two-flash fusion

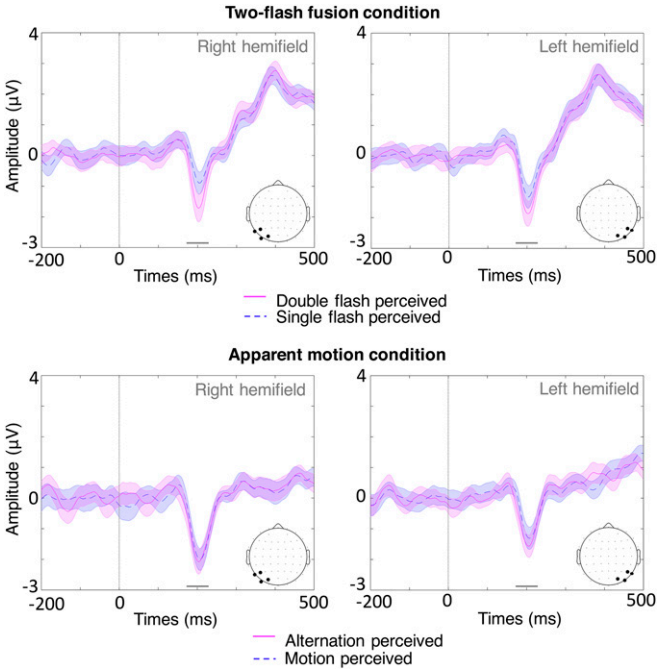

Fig. 2. Poststimulus neurophysiological signatures of integration/segregation over different TWs. ERPs locked to the onset of the first stimulus are shown for the two experimental conditions as a function of the stimulus presentation hemifield for the two-flash fusion trials (*Upper*) and the apparent motion trials (*Lower*). (*Insets*) Topographical maps depict the cluster of channels used for the analysis. The horizontal gray bar in the bottom part of each plot represents the time window used for the analysis of the N1 component (range: 180–220 ms).

condition and the apparent motion condition. Indeed, the highest decoding accuracy in predicting subjects' perceptual outcome from the phase of prestimulus oscillation in the two-flash fusion task was found for frequencies spanning predominantly the alpha band (~8–10 Hz) and around −400/−300 ms relative to the onset of the first stimulus (Fig. 3*A*; group average maximum decoding accuracy was observed in channel P6, mean = 52.88%, SD = 3.83). On the contrary, the highest decoding accuracy in predicting the perceptual outcome for the apparent motion condition was found for frequencies spanning predominantly the upper theta band (~6–7 Hz) at

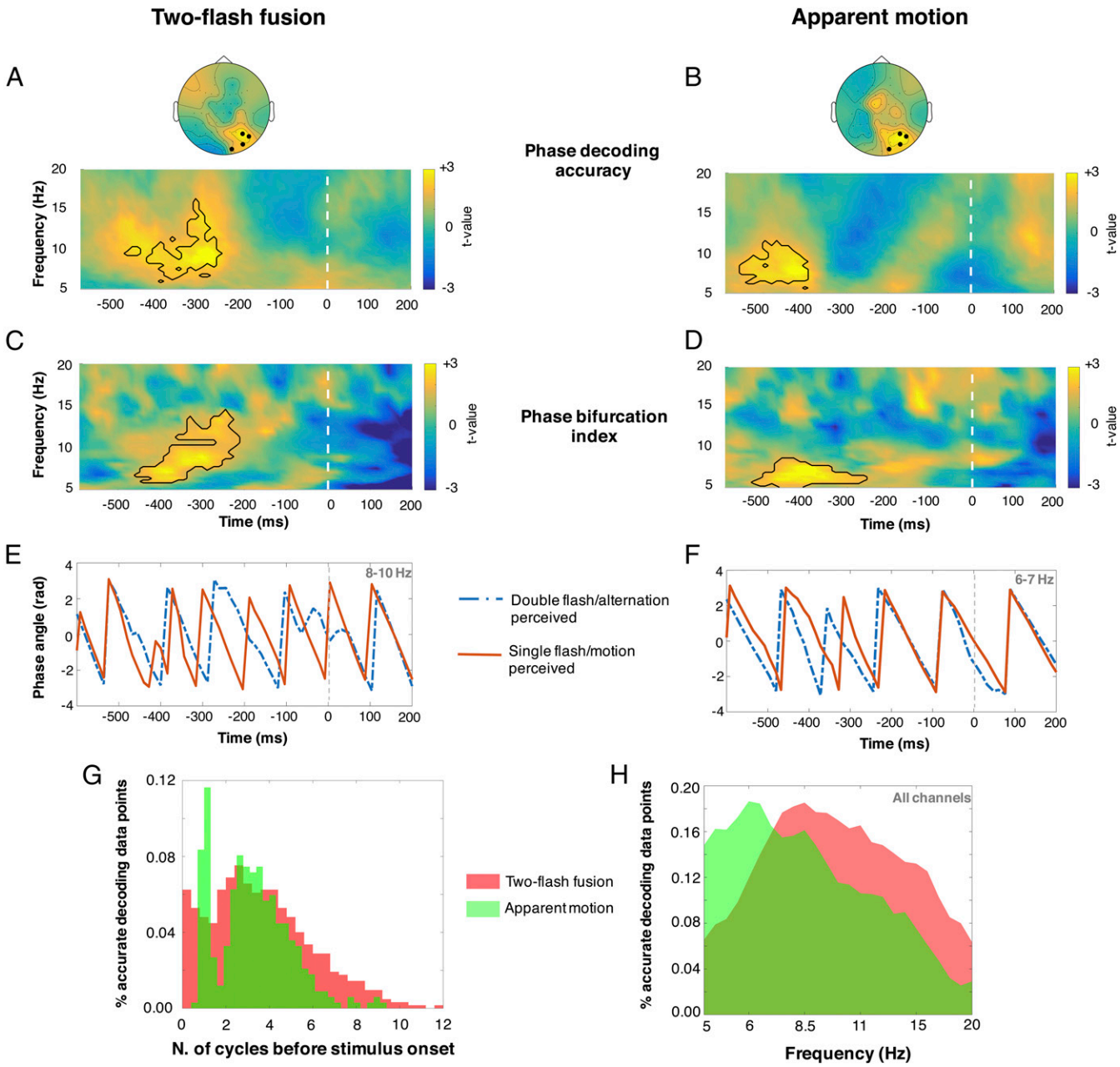

Fig. 3. Prestimulus/ongoing phase at different oscillatory rhythms predicts the temporal integration/segregation over different TWs. (*A* and *B*) Time frequency plots showing phase-decoding accuracy obtained with a naive Bayes classifier searchlight for the two types of trial (randomly appearing in the left or right visual hemifield). Color-coded t values represent the group-level difference against the chance level (50% decoding accuracy) as a function of the type of trial. The outlined areas of the plots delimit the intersection of time/frequency points in which a significant difference was obtained, with cluster-corrected permutation tests in the four right parieto-occipital channels showing maximum decoding accuracy (the channels are highlighted in the topographical maps above the time/frequency plots). (*C* and *D*) PBI data in which color-coded t values represent the group-level differences against PBI = 0 (no phase opposition). Also, in this case, the intersection of significant time/frequency points is outlined. (*E* and *F*) Phase-angle data averaged across trials and participants as a function of the perceptual outcome reported, which was either segregation (two flashes in the same or different positions) or integration (one single or moving flash). (*G*) Histogram showing the percentage of data points with a decoding accuracy significantly above chance for the entire time period of interest (−600/0 ms relative to the stimulus onset), expressed in terms of the number of cycles before the stimulus onset as a function of frequency. Note that the plots in all panels (except *H*) are related to the same right parieto-occipital cluster of channels showing the highest decoding accuracy in the prestimulus period. (*H*) Area plot showing the percentage of data points for the two types of trials showing a decoding accuracy significantly above chance in the entire time period of interest (−600/0 ms) as a function of frequency (on a logarithmic scale) in all EEG channels recorded.

around −500/−400 ms relative to the onset of the first stimulus (Fig. 3*B*; group average maximum decoding accuracy was observed in channel O2, mean = 53.17%, SD = 4.75). This pattern of results was not limited to the right parieto-occipital channels, but was a general pattern emerging also when looking at all recorded channels (Fig. 3*H*).

To control that these time/frequency effects were not contaminated by poststimulus ERP, we ran a simulation in which we applied a time/frequency transformation to a synthetic signal (i.e., sinusoidal wave mimicking an ERP with an onset time of 0 ms). As explained by Tallon-Baudry et al. (47), to determine the extent of temporal contamination caused by the wavelet, we calculated for each frequency the wavelet's temporal resolution σ_t, which is defined as twice the SD of the Gaussian envelope at a particular frequency. Using the same parameters that we used for our wavelet analysis (*Methods*), we found that the earliest contamination from poststimulus data points was at −210 ms for a signal at 5 Hz (i.e., the lowest frequency that was taken into account in our study). Since our significant results were found outside this time/frequency limit, we can be confident that no contamination from poststimulus data was present (Fig. S1).

Moreover, as evident in the histogram in Fig. 3*G*, when equating the time and frequency information and expressing the decoding accuracy instead in terms of number of cycles before the stimulus onset in which the ongoing phase was predictive of the perceptual outcome, we find substantial overlap between the two distributions. Most of the time/frequency points showing significantly accurate phase decoding were concentrated at around three cycles before the stimulus onset, a result that is examined further in *Discussion*.

Confirmation of these findings was also evident when looking at the results of the phase bifurcation index (PBI) (9) analyses (Fig. 3 *C* and *D*), where differences in phase were evaluated based on the intertrial coherence of the two different groups of trials (segregation vs. integration) as described in *Methods*. In the same cluster of channels, we found comparable results, with a PBI that was significantly above 0 (meaning significant phase opposition/difference between the two possible perceptual outcomes: segregation vs. integration) for time/frequency points that substantially overlapped those found with the naive Bayes classifier searchlight. Again, the two-flash trials showed significant results in the alpha range and apparent motion in the phase of the theta band.

It is worth noting that the analyses conducted so far are inappropriate for revealing effects that would systematically occur contralateral (or, possibly, ipsilateral) to the stimulus. This is because, for any EEG channel, these potential lateralized effects would only be present on half of the trials (when the stimulus is on the contralateral side). To overcome this issue, we performed a complementary analysis that involved "mirroring" all channels on half of the trials. Specifically, we mirrored channels for all trials containing stimuli appearing on the right hemifield. In this way, the effects that systematically occur contralaterally would map on the right electrodes and the ipsilateral effects would map on the left electrodes. We performed the same phase-decoding analyses described above, but no significant results emerged (two-flash fusion trials: all corrected $P > 0.142$, apparent motion trials: all corrected $P > 0.099$; Fig. S2).

Lastly, we ran a naive Bayes classifier searchlight on single-trial power values to check whether difference in power could partially explain the differences in the phase-decoding accuracy found for two-flash fusion and apparent motion trials. Results revealed only small differences in power in the cluster of right parieto-occipital channels, where phase-related differences emerged, which, importantly, did not overlap with the differences that emerged from the phase-decoding analysis (Fig. S3). This result confirms that phase-related differences were independent of power-related differences present in the ongoing oscillations.

Discussion

Perception simplifies the nature of the incoming sensory input in many different ways, such that information can be represented and stored in an optimized but more abstracted format. This process is well studied in the spatial domain (48, 49), but the way in which information is grouped together in the temporal domain is less clear. In the present study, we took advantage of different analysis methods, particularly of single-trial, multivariate EEG decoding of the subjects' perceptual outcome, to understand the relationship between the phase of the ongoing neural oscillation and temporal integration/segregation of stimuli over different TWs. Indeed, mounting evidence shows that the ongoing oscillations in the theta/alpha bands are not only related to trial-by-trial fluctuations in threshold-level perception in different sensory modalities (9, 10, 12, 14–16) but also predict temporal segregation/integration of visual stimuli over time (8, 34–37). These findings are in agreement with the idea that the phase of neural oscillations reflects modulation of cortical excitability (28–31).

In the present study, we show that the way in which ongoing neural oscillations determine whether visual information is temporally integrated or segregated does not depend on a single, general sampling rhythm. On the contrary, different ongoing oscillatory rhythms determine the temporal integration/segregation of stimuli over time according to the TW involved. We found that when participants were presented with a bistable stimulus comprising two distinct flashes in the same spatial position and separated by an ISI of 40 ms (two-flash fusion trials), the subjective interpretation of this bistable stimulus (one flash vs. two flashes perceived) could be accurately decoded from the phase of the ongoing oscillation within the alpha band (maximum decoding accuracy at around 8–10 Hz). On the other hand, when participants were presented with a bistable stimulus comprising two distinct flashes appearing in different spatial positions and separated by an ISI of 120 ms (apparent motion trials), the subjective interpretation of this bistable stimulus (motion vs. alternation) could be accurately decoded from the phase of the ongoing oscillation within the theta band (maximum decoding accuracy at around 6–7 Hz). These results renewed previous evidence (8, 35) of a relationship between the alpha phase and timing in perception. In particular, a previous study examining the "flash-lag" effect (50), a spatiotemporal illusion where a continuously moving object is incorrectly perceived ahead of its true location when an event (e.g., flash) appears, found that the magnitude of the effect varied along with the ongoing 5- to 20-Hz EEG phase. Those results suggested that neural periodicity is involved in the flash-lag illusion.

Additionally, the present results are in agreement with recent studies from our own and other laboratories providing evidence for a causal link between neural oscillations and spatiotemporal aspects of perception (51, 52). In a recent study, we employed sensory entrainment in the prestimulus interval to align ongoing oscillations to a theta, alpha, or beta rhythm. We found that the frequency of temporal segregation was modified by sensory entrainment at the theta and alpha (but not beta) rhythms (52). Another recent study employing an illusory jitter perception termed the "motion-induced spatial conflict" showed that the illusory visual vibrations mirror the intrinsic peak alpha frequency of the participants. Moreover, a temporary shift of the individual alpha peak due to alternate current stimulation altered the perceived jitter frequency (51).

The phase effect we found could not be dependent on variations in oscillatory amplitude, as our analyses demonstrated, thus suggesting that at least for the alpha/theta band, the phase of ongoing neural oscillations could impact stimulus processing independently from amplitude variations, in agreement with previous evidence (35). Multivariate decoding revealed also that the topography of the effect was comparable for the two types of trial, with the highest decoding accuracy visible in right parieto-occipital channels, suggesting a common area/network responsible for temporal sampling across different time periods. Although EEG

does not allow for the definition of exact underlying neural sources, the right parieto-occipital topography revealed by our multivariate decoding analysis is in agreement with mounting evidence showing that the neural sources underlying the modulation of the ongoing theta/alpha phase are linked to the activity of the right posterior parietal cortex (PPC) (12, 53–55). Hanslmayr et al. (12), for example, show that the underlying modulation of perception operated by the phase of ongoing oscillations reflects the bidirectional information flow between the occipital cortex and right PPC, suggesting that the oscillatory phase reflects the periodic gate of perception by opening transient time periods in which long-distance cortical information transfer can take place. Similarly, the tendency to either integrate or segregate two visual stimuli in time has been linked to right parieto-occipital sources (36).

Overall, the present findings suggest a precise mapping between oscillatory activity at a specific frequency and the temporal organization of sensory input into coherent percepts. Variations in the theta and alpha (and maybe other) oscillatory rhythms, reflecting periods of increased/decreased excitability, would determine if subsequent stimuli are perceived in their "real" nature, and thus as distinct events, or if they are subjected to some forms of temporal averaging that lead to a relatively "poorer" quality of processing (i.e., perception of a single flash in the case of the two-flash fusion trials and perception of a single moving flash in apparent motion trials).

It is interesting to observe that the number of oscillatory cycles from which subjective perception can be efficiently decoded largely converges around three cycles before the onset of the stimulus, independent of the specific oscillatory rhythms involved. This timing is consistent with the idea that the presence of target-evoked ERPs and signal filtering involved in commonly used time/frequency analyses (e.g., wavelet) causes a shift of the maximum phase difference toward earlier time points (56). That result suggests that the phase modulation found in this study may have its true latency around the time of the stimulus presentation.

Although a direct link between the temporal organization of perception (into discrete units) and oscillations has been suggested for some time (5–8, 57, 58), this idea has remained controversial theoretically and has been repeatedly challenged empirically. The current findings may provide some assistance in resolving this controversy. The finding of two different perceptual TWs mapping onto two different frequency bands may help to explain the lack of consistent evidence for a single, master frequency of temporal resolution. Indeed, in addition to the alpha band, neural correlates of TWs have been reported in theta and beta frequencies (reviewed in ref. 58).

On a more theoretical level, there is a long-standing debate between "perceptual moment" and "continuous perception" descriptions of the phenomenology of visual perception, as captured by James' idea of a stream of conscious awareness (59). It has been argued that the presence of discrete TWs in sensory processing does not necessarily signify that perception is discontinuous (44–46). A hierarchy of different TWs would potentially mask the discontinuities of TWs at a lower stage. For example, the Nyquist–Shannon theorem shows how discrete samples can be transformed back into a continuous function through the use of multiple sampling frequencies, such as a combination of theta and alpha frequencies. Such a hierarchy of TWs may contribute to the intuitive impression of a continuous flow despite discrete sensory sampling mechanisms. Moreover, the presence of multiple sampling frequencies would help to balance the needs of temporal integration (i.e., to improve perceptual decision making by combining information over time) and sensitivity to changes in input that reflect new events in a dynamic environment. In the case of language, it is clear that auditory processing takes place for different TWs ranging from phonemes (tens of milliseconds) to syllables (hundreds of milliseconds), to words and phrases (seconds). Recent studies have linked these auditory TWs to oscillatory behavior, with shaping and entrainment of these frequencies to the specific speech patterns of speakers (60). Likewise, visual events occur over different time periods, which might require multiple visual TWs in a sort of language of vision.

A number of oscillatory frequencies have been linked to different, specific aspects of perceptual processing. For example, theta-band rhythms have been linked to the grouping of sensory inputs into meaningful, temporal chunks that incorporate information across multiple brain regions (36, 61, 62), whereas gamma oscillations may reflect more local, bottom-up processing and beta oscillations may reflect more feedback and top-down control (63, 64). The current results would be consistent with distinct roles for alpha in determining temporal resolution (8, 58, 65, 66) and for theta-frequency sampling in generating more complex, meaningful percepts of objects and events (36, 62). In terms of the mechanisms by which these two frequencies diverge, one possibility could be that when perception depends on higher order areas or larger networks (e.g., networks involving primary visual areas, but also motion processing and attentional control areas), a slower rhythm would emerge as a result of stronger feedback projections and longer interareal communication time among these regions (61).

To conclude, in the present study, we took advantage of a method using phase information for multivariate decoding of the perceptual outcome, and we demonstrate within a single study that the perceptual sampling of visual events over different temporal scales does not rely on a single sampling mechanism but, instead, on the phase of different oscillatory rhythms. The presence of multiple TWs and their mapping into different oscillatory rhythms may help to explain why discrete sensory processing does not result in discontinuity of perception.

Methods

Participants. Twenty-seven adult participants (mean age = 24 y, SD = 3, 11 males) recruited at the University of Trento took part in the present study as paid volunteers. From this original sample of participants, three subjects were removed for the EEG analysis because of noisy data in the prestimulus period, leaving 24 participants for the full analysis. All participants provided informed consent, had normal or corrected-to-normal vision, and reported normal hearing. They reported no history of neurological disorders. The study was approved by the Ethics Committee of the Center for Mind/Brain Sciences at the University of Trento and conforms to the principles elucidated in the Declaration of Helsinki of 2013.

Stimuli, Procedure, and Data Analysis. Detailed information can be found in *SI Methods*.

ACKNOWLEDGMENTS. This research was supported by a European Research Council grant, "Construction of Perceptual Space-Time" (StG Agreement 313658).

1. Hirsh IJ, Sherrick CE, Jr (1961) Perceived order in different sense modalities. *J Exp Psychol* 62:423–432.
2. Wertheimer M (1912) Experimentelle studium uber das sehen von bewegung. *Z Psychol Z Angew Psychol* 61:161–265. German.
3. Finlay D, von Grünau M (1987) Some experiments on the breakdown effect in apparent motion. *Percept Psychophys* 42:526–534.
4. Breitmeyer B, Öğmen H (2006) *Visual Masking: Time Slices Through Conscious and Unconscious Vision* (Oxford Univ Press, Oxford, UK).
5. Bishop GH (1932) Cyclic changes in excitability of the optic pathway of the rabbit. *Am J Physiol* 103:213–224.
6. Lansing RW (1957) Relation of brain and tremor rhythms to visual reaction time. *Electroencephalogr Clin Neurophysiol* 9:497–504.
7. Stroud JM (1967) The fine structure of psychological time. *Ann N Y Acad Sci* 138: 623–631.
8. Varela FJ, Toro A, John ER, Schwartz EL (1981) Perceptual framing and cortical alpha rhythm. *Neuropsychologia* 19:675–686.
9. Busch NA, Dubois J, VanRullen R (2009) The phase of ongoing EEG oscillations predicts visual perception. *J Neurosci* 29:7869–7876.
10. Fiebelkorn IC, Saalmann YB, Kastner S (2013) Rhythmic sampling within and between objects despite sustained attention at a cued location. *Curr Biol* 23:2553–2558.

11. Fiebelkorn IC, et al. (2013) Cortical cross-frequency coupling predicts perceptual outcomes. *Neuroimage* 69:126–137.
12. Hanslmayr S, Volberg G, Wimber M, Dalal SS, Greenlee MW (2013) Prestimulus oscillatory phase at 7 Hz gates cortical information flow and visual perception. *Curr Biol* 23:2273–2278.
13. Nunn CM, Osselton JW (1974) The influence of the EEG alpha rhythm on the perception of visual stimuli. *Psychophysiology* 11:294–303.
14. Mathewson KE, Gratton G, Fabiani M, Beck DM, Ro T (2009) To see or not to see: Prestimulus alpha phase predicts visual awareness. *J Neurosci* 29:2725–2732.
15. Ng BS, Schroeder T, Kayser C (2012) A precluding but not ensuring role of entrained low-frequency oscillations for auditory perception. *J Neurosci* 32:12268–12276.
16. Strauß A, Henry MJ, Scharinger M, Obleser J (2015) Alpha phase determines successful lexical decision in noise. *J Neurosci* 35:3256–3262.
17. Callaway E, 3rd, Yeager CL (1960) Relationship between reaction time and electroencephalographic alpha phase. *Science* 132:1765–1766.
18. Dustman RE, Beck EC (1965) Phase of alpha brain waves, reaction time and visually evoked potentials. *Electroencephalogr Clin Neurophysiol* 18:433–440.
19. Drewes J, VanRullen R (2011) This is the rhythm of your eyes: The phase of ongoing electroencephalogram oscillations modulates saccadic reaction time. *J Neurosci* 31: 4698–4708.
20. Busch NA, VanRullen R (2010) Spontaneous EEG oscillations reveal periodic sampling of visual attention. *Proc Natl Acad Sci USA* 107:16048–16053.
21. Landau AN, Schreyer HM, van Pelt S, Fries P (2015) Distributed attention is implemented through theta-rhythmic gamma modulation. *Curr Biol* 25:2332–2337.
22. Dugué L, Marque P, VanRullen R (2015) Theta oscillations modulate attentional search performance periodically. *J Cogn Neurosci* 27:945–958.
23. Buschman TJ, Miller EK (2009) Serial, covert shifts of attention during visual search are reflected by the frontal eye fields and correlated with population oscillations. *Neuron* 63:386–396.
24. Jansen BH, Brandt ME (1991) The effect of the phase of prestimulus alpha activity on the averaged visual evoked response. *Electroencephalogr Clin Neurophysiol* 80: 241–250.
25. Scheeringa R, Mazaheri A, Bojak I, Norris DG, Kleinschmidt A (2011) Modulation of visually evoked cortical FMRI responses by phase of ongoing occipital alpha oscillations. *J Neurosci* 31:3813–3820.
26. Gruber WR, et al. (2014) Alpha phase, temporal attention, and the generation of early event related potentials. *Neuroimage* 103:119–129.
27. Dugué L, Marque P, VanRullen R (2011) The phase of ongoing oscillations mediates the causal relation between brain excitation and visual perception. *J Neurosci* 31: 11889–11893.
28. Klimesch W, Sauseng P, Hanslmayr S (2007) EEG alpha oscillations: The inhibition-timing hypothesis. *Brain Res Brain Res Rev* 53:63–88.
29. Jensen O, Mazaheri A (2010) Shaping functional architecture by oscillatory alpha activity: Gating by inhibition. *Front Hum Neurosci* 4:186.
30. Jensen O, Bonnefond M, VanRullen R (2012) An oscillatory mechanism for prioritizing salient unattended stimuli. *Trends Cogn Sci* 16:200–206.
31. Jensen O, Gips B, Bergmann TO, Bonnefond M (2014) Temporal coding organized by coupled alpha and gamma oscillations prioritize visual processing. *Trends Neurosci* 37: 357–369.
32. Haegens S, Nácher V, Luna R, Romo R, Jensen O (2011) α-Oscillations in the monkey sensorimotor network influence discrimination performance by rhythmical inhibition of neuronal spiking. *Proc Natl Acad Sci USA* 108:19377–19382.
33. Haegens S, et al. (2015) Laminar profile and physiology of the α rhythm in primary visual, auditory, and somatosensory regions of neocortex. *J Neurosci* 35:14341–14352.
34. Mathewson KE, et al. (2012) Making waves in the stream of consciousness: Entraining oscillations in EEG alpha and fluctuations in visual awareness with rhythmic visual stimulation. *J Cogn Neurosci* 24:2321–2333.
35. Milton A, Pleydell-Pearce CW (2016) The phase of pre-stimulus alpha oscillations influences the visual perception of stimulus timing. *Neuroimage* 133:53–61.
36. Wutz A, Muschter E, van Koningsbruggen MG, Weisz N, Melcher D (2016) Temporal integration windows in neural processing and perception aligned to saccadic eye movements. *Curr Biol* 26:1659–1668.
37. Wutz A, Weisz N, Braun C, Melcher D (2014) Temporal windows in visual processing: "Prestimulus brain state" and "poststimulus phase reset" segregate visual transients on different temporal scales. *J Neurosci* 34:1554–1565.
38. Drewes J, Zhu W, Wutz A, Melcher D (2015) Dense sampling reveals behavioral oscillations in rapid visual categorization. *Sci Rep* 5:16290.
39. Pöppel E (1997) A hierarchical model of temporal perception. *Trends Cogn Sci* 1: 56–61.
40. Pöppel E (2009) Pre-semantically defined temporal windows for cognitive processing. *Philos Trans R Soc Lond B Biol Sci* 364:1887–1896.
41. Hasson U, Yang E, Vallines I, Heeger DJ, Rubin N (2008) A hierarchy of temporal receptive windows in human cortex. *J Neurosci* 28:2539–2550.
42. Fairhall SL, Albi A, Melcher D (2014) Temporal integration windows for naturalistic visual sequences. *PLoS One* 9:e102248.
43. Wang L, et al. (2016) Scanning the world in three seconds: Mismatch negativity as an indicator of temporal segmentation. *PsyCh J* 5:170–176.
44. van de Grind W (2002) Physical, neural, and mental timing. *Conscious Cogn* 11: 241–264, discussion 308–313.
45. van Wassenhove V (2009) Minding time in an amodal representational space. *Philos Trans R Soc Lond B Biol Sci* 364:1815–1830.
46. Busch N, VanRullen R (2014) Is visual perception like a continuous flow or a series of snapshots. *Subjective Time: The Philosophy, Psychology, and Neuroscience of Temporality* (MIT Press Cambridge, MA), pp 161–178.
47. Tallon-Baudry C, Bertrand O, Delpuech C, Pernier J (1996) Stimulus specificity of phase-locked and non-phase-locked 40 Hz visual responses in human. *J Neurosci* 16: 4240–4249.
48. Alvarez GA (2011) Representing multiple objects as an ensemble enhances visual cognition. *Trends Cogn Sci* 15:122–131.
49. Whitney D, Yamanashi Leib A (September 11, 2017) Ensemble perception. *Annu Rev Psychol*, 10.1146/annurev-psych-010416-044232.
50. Chakravarthi R, Vanrullen R (2012) Conscious updating is a rhythmic process. *Proc Natl Acad Sci USA* 109:10599–10604.
51. Minami S, Amano K (2017) Illusory jitter perceived at the frequency of alpha oscillations. *Curr Biol* 27:2344–2351.e4.
52. Ronconi L, Melcher D (2017) The role of oscillatory phase in determining the temporal organization of perception: Evidence from sensory entrainment. *J Neurosci* 37: 10636–10644.
53. van Dijk H, Schoffelen JM, Oostenveld R, Jensen O (2008) Prestimulus oscillatory activity in the alpha band predicts visual discrimination ability. *J Neurosci* 28:1816–1823.
54. Thut G, et al. (2011) Rhythmic TMS causes local entrainment of natural oscillatory signatures. *Curr Biol* 21:1176–1185.
55. Jaegle A, Ro T (2014) Direct control of visual perception with phase-specific modulation of posterior parietal cortex. *J Cogn Neurosci* 26:422–432.
56. Brüers S, VanRullen R (2017) At what latency does the phase of brain oscillations influence perception? *eNeuro* 4:e0078-17.2017.
57. VanRullen R, Koch C (2003) Is perception discrete or continuous? *Trends Cogn Sci* 7: 207–213.
58. VanRullen R (2016) Perceptual cycles. *Trends Cogn Sci* 20:723–735.
59. James W (1890) *Principles of Psychology* (Holt, New York).
60. ten Oever S, Sack AT (2015) Oscillatory phase shapes syllable perception. *Proc Natl Acad Sci USA* 112:15833–15837.
61. Dugué L, VanRullen R (2017) Transcranial magnetic stimulation reveals intrinsic perceptual and attentional rhythms. *Front Neurosci* 11:154.
62. Schroeder CE, Lakatos P (2009) Low-frequency neuronal oscillations as instruments of sensory selection. *Trends Neurosci* 32:9–18.
63. Engel AK, Fries P (2010) Beta-band oscillations–Signalling the status quo? *Curr Opin Neurobiol* 20:156–165.
64. Buschman TJ, Miller EK (2007) Top-down versus bottom-up control of attention in the prefrontal and posterior parietal cortices. *Science* 315:1860–1862.
65. Cecere R, Rees G, Romei V (2015) Individual differences in alpha frequency drive crossmodal illusory perception. *Curr Biol* 25:231–235.
66. Samaha J, Postle BR (2015) The speed of alpha-band oscillations predicts the temporal resolution of visual perception. *Curr Biol* 25:2985–2990.

Supporting Information

Ronconi et al. 10.1073/pnas.1714522114

SI Methods

Stimuli, Apparatus, and Procedure. All visual stimuli were displayed on a 22.5-inch VIEWPixx monitor with a vertical refresh rate of 100 Hz. The target stimuli (hereafter "flashes") were luminance-defined Gaussian blobs sized 0.5° × 0.5°. The contrast of the flashes was individually adjusted before the experiment to ensure that the stimulus was presented well above threshold. We first determined with a QUEST procedure the absolute contrast threshold (mean Michelson contrast threshold between the flash and the background was 9.02%). The resulted contrast value was then multiplied by a factor of 1.5 or 2 depending on participants' performance during a practice block entailing the same stimuli that were subsequently used in the experiment. Specifically, to be sure that we were employing the lowest suprathreshold contrast value that could ensure the correct detection of the presentation of a stimulus during the experiment (no misses), we chose the lowest multiplication factor (1.5, 2, or 2.5) of the absolute contrast threshold value at which participants were able to detect the stimulus (either as one flash or two flashes) in all of the 20 trials of the practice block. Following this procedure, the average Michelson contrast value between the flash and the background was 15.34%. Critically, we chose to use relatively weak flashes to increase our sensitivity to the effects of ongoing oscillations. Indeed, a very high contrast stimulus might itself create a full phase reset, and thus decrease the influence of prestimulus, ongoing oscillations. In other words, the ongoing oscillatory activity would be perturbed by a strong stimulus, and any difference in the nature of the oscillation (e.g., frequency, scalp location) between the two types of temporal integration/segregation tested here would be masked. At the same time, the choice of stimuli well above threshold was motivated by the need to avoid issues of detecting the presence or lack of presence of stimuli. Indeed, as reviewed in the Introduction, many studies report an effect of the phase of the ongoing oscillations in determining the detection of stimuli at threshold. Instead, our interest here was in studying whether ongoing oscillations could determine the integration/segregation of suprathreshold stimuli over time. The experiment was programmed in MATLAB (MathWorks, Inc.), using the Psychtoolbox (1), and all visual stimuli were displayed on a gray background (halfway between white and black).

Experimental Design. The stimulus presentation methodology is illustrated in Fig. 1. All trials started with the onset of a fixation point for a variable presentation time (ranging from 1,350 to 1,750 ms). Each of the two target flashes had a duration of 10 ms (one refresh rate). In the two-flash fusion trials, the two target flashes were displayed in the same position in the left or right hemifield at 6° of eccentricity from the fixation, aligned to the horizontal axis. The stimulus presentation hemifield was randomized across trials, and the two flashes were always separated by an ISI of 40 ms (four refresh cycles). In the apparent motion trials, the first of the two target flashes was always displayed at 6° of eccentricity in the left or right hemifield and aligned to the horizontal axis. The second target flash was displayed after an ISI of 120 ms (12 refresh rate) above or below the position of the first flash (at a distance of 4°) at the same eccentricity and in the same hemifield.

The ISI values for the two types of trials were chosen based on pilot experiments, showing that these time intervals were optimal to obtain in both cases a bistable stimulus that, despite being physically constituted by two distinct flashes, was sometimes perceived as one static or moving flash and sometimes as two flashes alternating in the same or different spatial positions. After stimuli presentation, a blank screen of 1,500 ms appeared, followed by the response screen, in which participants were asked to report if they perceived one or two flashes for two-flash fusion trials or if they perceived motion or alternation (and in which direction: upward or downward) for apparent motion trials. Participants were asked to respond at their own pace with no time constraints. After the response screen, an intertrial interval of 1,000 ms anticipated the following trial.

The total number of trials administered for each participant was 1,200, consisting of 540 bistable trials for the two-flash fusion task and 540 bistable trials for the apparent motion task. Moreover, 60 "catch" trials with longer ISIs were presented for both trial types (100 ms for the two-flash fusion task and 200 ms for the apparent motion task). The different types of trial were randomly intermixed and split into smaller blocks to prevent fatigue. All participants were unaware of the fact that bistable trials were all identical.

EEG Recording and Preprocessing. EEG data were recorded from a 64-channel system for ac/dc recordings (Brain Products GmbH) in an electrically shielded booth at a sampling rate of 500 Hz. Electrodes were positioned at the following scalp sites: Fpz, Fp1, Fp2, AF7, AF3, AF4, AF8, F7, F5, F3, F1, Fz, F2, F4, F6, F8, FT7, FC5, FC3, FC1, FCz, FC2, FC4, FC6, FT8, T7, C5, C3, C1, Cz, C2, C4, C6, T8, TP9, TP7, CP5, CP3, CP1, CPz, CP2, CP4, CP6, TP8, TP10, P7, P5, P3, P1, Pz, P2, P4, P6, P8, PO7, PO3, POz, PO4, PO8, O1, Oz, and O2. Moreover, for measuring the vertical and horizontal electrooculograms, activity was recorded also from two electrodes placed below one eye and on the external canthus. All electrodes were online-referenced to Cz. Spherical interpolation was carried out on individual bad channels if required (average number of interpolated channels: 0.44, range: 1–5). Offline, data were preprocessed as follows: Data were down-sampled to 250 Hz, rereferenced to an average reference, band pass-filtered between 0.1 and 80 Hz, and epoched between −1,500 and 1,000 ms relative to the onset of the first flash. An independent component analysis was used to correct for electrooculographic artifacts unless they occurred right before the stimulus onset, because the epochs were excluded in this case. Additionally, epochs containing voltage deviations exceeding ±150 μV or contaminated by muscular artifacts were excluded. The remaining artifact-free epochs (average rate of accepted epochs per participants = 94.56%, SD = 4.78) were transformed into the time/frequency domain using a complex Morlet wavelet with a varying number of cycles (three at the lowest frequency and 10 at the highest frequency) to obtain time/frequency (complex number) representation in 50 log-spaced frequency points from 3 to 50 Hz and 100 time points ranging from −944 to 440 ms relative to the stimulus onset. Data analysis was performed using MATLAB, EEGLAB (2), and CoSMoMVPA (3).

EEG Data Analysis: ERPs. Neurophysiological signatures of integration and segregation of the two flashes were assessed by analyzing the ERPs locked to the onset of the first stimulus. To accomplish this goal, we used smaller epochs (−200/500 ms) and a baseline correction of the time period before the stimulus onset (−200/0 ms). ERPs were analyzed in a cluster of parieto-occipital channels contralateral to the stimulus onset (Left: P5, P7, PO3, and PO7; Right: P6, P6, PO4, and PO8). The mean amplitudes of the P1 (140–180 ms) and N1 (180–220 ms) ERP components were extracted and analyzed, separately for the two trial types, with a repeated measure ANOVA with the following within-subject factors: two outcomes (segregation/integration), two stimulus hemifields (left/right), and two ROIs (ipsilateral/contralateral).

EEG Data Analysis: Single-Trial Phase Decoding and Overall Phase Difference (PBI). For the phase classification, we used for each participant a searchlight with a cross-validated naive Bayes phase classifier (as implemented in the CoSMoMVPA toolbox: www.cosmomvpa.org/). For the cross-validation, we used a split-half method: 50% of the trials were selected pseudorandomly for training the classifier, and the remaining 50% were used for testing. We performed this operation twice, training on half and testing on the other half, and vice versa. Classification accuracy was computed as the number of correctly predicted condition labels divided by the total number of predictions. In all cases, the train and test sets were both balanced across the two conditions (integration or segregation). In other words, the number of trials in each condition was the same; where necessary, some trials (on average, 20% of the total trials) were dropped from the train or test set to ensure balance.

For the classifier, we used a custom (faster) reimplementation of some of the functionality present in the MATLAB Toolbox for Circular Statistics (4) (https://www.jstatsoft.org/article/view/v031i10). We used a multivariate phase classification approach as follows. The input of the classifier was phase data from a set of trials with two conditions for a set of k features (combination of time points, frequencies, and channels). For each condition label c (indicating integration or segregation) and feature i in the training set, the average phase $\theta_{c,i}$ and concentration parameter $\kappa_{c,i}$ were computed. For each trial in the test set, the probability $p_{i,c}$ that it belonged to class c according to feature i was computed using the von Mises circular probability density function (as implemented in circ_vmpdf.m in the CircStat toolbox). Since our classification approach was naive Bayes (assuming independence across features), the combined class probability P_c that a trial belonged to condition c was computed as $P_c = p_{1,c} * p_{2,c} * \ldots p_{k,c}$, integrating the information across the k features. The predicted condition label was set to the one with the highest probability. For improved accuracy when using very small probability values, our implementation took the logarithm of the probabilities and summed them. Note that since we used balanced trial counts for the two conditions there was no need to assume different prior probabilities accounting for class frequency.

For the spatiotemporal-frequency searchlight, each searchlight used three channels and was based on radii of four time points and eight frequencies. For a given "center" feature (combination of channel, time point, and frequency), features from the nearest three channels (including itself) that were within a distance of four time points and eight frequencies were selected and used for cross-validated classification as described earlier. The classification accuracy was then assigned to the center feature. This process was repeated for each feature, resulting in a classification accuracy map for all channels, time points, and frequency bins.

To corroborate results from the single-trial phase-decoding analyses, we analyzed the average phase difference between the trial outcome (segregation vs. integration), separately for the two types of trials, employing the phase bifurcation index (PBI). The PBI was introduced by Busch et al. (5) and employed in numerous subsequent studies (reviewed in ref. 6). For the PBI calculation, we first computed phase coherence across trials with the intertrial phase coherence [ITC; also called phase-locking factor (7, 8)] as follows:

$$\mathrm{ITC} = \left| \sum_{i=1:n} \frac{\omega_i}{|\omega_i|} \right| / n. \qquad \textbf{[S1]}$$

In Eq. **S1**, ω_i is the complex number [with $|\omega_i|$ and angle(ω_i) representing the oscillatory amplitude and phase, respectively] for each trial i. The ITC measure can have values between 0 and 1, with 0 representing the absence of synchronization across trials relative to the time-locking event and a value of 1 indicating perfect synchronization. To calculate the phase difference between correct and incorrect trials for both the strong and mid-crowding conditions, we calculated the PBI as follows:

$$\mathrm{PBI} = (\mathrm{ITC}_{\mathrm{SEGREGATION}} - \mathrm{ITC}_{\mathrm{ALL}}) \times (\mathrm{ITC}_{\mathrm{INTEGRATION}} - \mathrm{ITC}_{\mathrm{ALL}}). \qquad \textbf{[S2]}$$

In our case, the $\mathrm{ITC}_{\mathrm{ALL}}$ was calculated taking all trials within the two-flash fusion and the apparent motion condition, independent from the trial outcome. PBI values can range from −1 to 1. When the phases of the two trial groups (segregation vs. integration in our case) are concentrated at different phase angles, the PBI will have a positive value, with an upper hypothetical bound of 1, indicating perfect phase locking in both conditions (ITC = 1), but at opposite phases (thus combined with an overall phase-locking ITC = 0). On the contrary, the null hypothesis of random phase distributions for correct and incorrect trials predicts a PBI value close to 0. Finally, when only one condition exhibits significant phase locking, while the other exhibits a random phase distribution, PBI values are negative. Since the reliability of ITC (and consequently of the PBI) is dependent on trial number (9, 10), we computed for each participant the PBI and subsequent phase analyses on a number of trials equal to the total number of trials in the condition with fewer trials.

Statistical Analyses of EEG Phase Decoding and PBI. For the main analysis of single-trial phase decoding, statistical analyses were used at the group level to assess whether the decoding accuracy was significantly above chance (i.e., 50%, given that the decoding was performed between two outcomes: segregation vs. integration) for all times/frequencies/channels tested. Specifically, we used nonparametric permutation tests (number of iterations = 10,000) with cluster-based correction (11) for multiple comparisons (maximum sum statistic setting the threshold P value to $\alpha = 0.05$, one-tailed) applied in the 3D space of all time points, channels (excluding electrooculogram channels), and frequencies.

In cases in which a significant decoding accuracy was found (i.e., significantly above chance), we additionally analyzed PBI at the group level in the same cluster of channels. Specifically, we used once again cluster-corrected permutation tests (two-tailed in this case) as described above to assess whether the PBI values of all prestimulus time points and frequencies were significantly different from 0 (indeed, random phase distributions for correct and incorrect trials predict a PBI equal to 0), similar to what has been done in previous studies (e.g., refs. 12–14).

Both analyses were restricted to frequencies ranging from 5 to 20 Hz and to time points ranging from −600 to 0 ms relative to the stimulus.

EEG Data Analysis: Single-Trial Power Decoding and Relative Statistical Analyses. For the power classification, we used in each participant a searchlight with a cross-validated naive Bayes phase classifier with the same procedure described above. The only difference was that for the power analysis, the naive Bayes classifier assumed a Gaussian (normal) distribution (for this reason, it is also called a Gaussian naive Bayes classifier), as implemented in the CoSMoMVPA toolbox (www.cosmomvpa.org/; see cosmo_naive_bayes_classifier_searchlight.m). Afterward, statistical analyses on decoding accuracy were performed with the same procedure described above.

1. Iemi L, Chaumon M, Crouzet SM, Busch NA (2017) Spontaneous neural oscillations bias perception by modulating baseline excitability. *J Neurosci* 37:807–819.
2. Delorme A, Makeig S (2004) EEGLAB: An open source toolbox for analysis of single-trial EEG dynamics including independent component analysis. *J Neurosci Methods* 134:9–21.
3. Oosterhof NN, Connolly AC, Haxby JV (2016) CoSMoMVPA: Multi-modal multivariate pattern analysis of neuroimaging data in Matlab/GNU octave. *Front Neuroinform* 10:27.
4. Berens P (2009) CircStat: A MATLAB toolbox for circular statistics. *J Stat Softw* 31:1–21.
5. Busch NA, Dubois J, VanRullen R (2009) The phase of ongoing EEG oscillations predicts visual perception. *J Neurosci* 29:7869–7876.
6. VanRullen R (2016) How to evaluate phase differences between trial groups in ongoing electrophysiological signals. *Front Neurosci* 10:426.
7. Tallon-Baudry C, Bertrand O, Delpuech C, Pernier J (1996) Stimulus specificity of phase-locked and non-phase-locked 40 Hz visual responses in human. *J Neurosci* 16:4240–4249.
8. Lachaux JP, Rodriguez E, Martinerie J, Varela FJ (1999) Measuring phase synchrony in brain signals. *Hum Brain Mapp* 8:194–208.
9. Vinck M, van Wingerden M, Womelsdorf T, Fries P, Pennartz CM (2010) The pairwise phase consistency: A bias-free measure of rhythmic neuronal synchronization. *Neuroimage* 51:112–122.
10. Moratti S, Clementz BA, Gao Y, Ortiz T, Keil A (2007) Neural mechanisms of evoked oscillations: Stability and interaction with transient events. *Hum Brain Mapp* 28:1318–1333.
11. Maris E, Oostenveld R (2007) Nonparametric statistical testing of EEG- and MEG-data. *J Neurosci Methods* 164:177–190.
12. Strauß A, Henry MJ, Scharinger M, Obleser J (2015) Alpha phase determines successful lexical decision in noise. *J Neurosci* 35:3256–3262.
13. Wutz A, Muschter E, van Koningsbruggen MG, Weisz N, Melcher D (2016) Temporal integration windows in neural processing and perception aligned to saccadic eye movements. *Curr Biol* 26:1659–1668.
14. Ronconi L, Bellacosa Marotti R (2017) Awareness in the crowd: Beta power and alpha phase of prestimulus oscillations predict object discrimination in visual crowding. *Conscious Cogn* 54:36–46.
15. Iemi L, Chaumon M, Crouzet SM, Busch NA (2017) Spontaneous neural oscillations bias perception by modulating baseline excitability. *J Neurosci* 37:807–819.

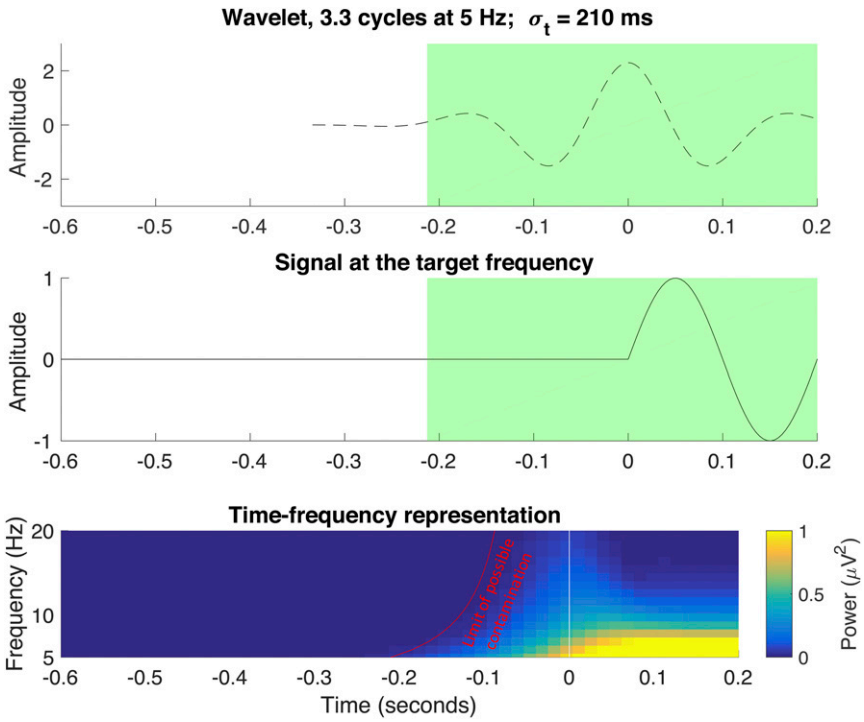

Fig. S1. Representation of a simulation in which we applied a time/frequency transformation to an ideal ERP waveform. As explained by Tallon-Baudry et al. (7) and Iemi et al. (15), to determine the extent of temporal contamination caused by the wavelet, we calculated for each frequency the wavelet's temporal resolution σ_t, which is defined as twice the SD of the Gaussian envelope at a particular frequency. We found that the earliest contamination possibly occurring from poststimulus data points in our study was at 210 ms before the stimulus onset for a signal at 5 Hz (the lowest frequency that was taken into account in our study). In the plot, this is represented by the green shaded area (*Upper* and *Middle*) or by the lowest point of the red curve (*Lower*). Since our significant results were found outside this time/frequency limit, we can be confident that no contamination from poststimulus data were present.

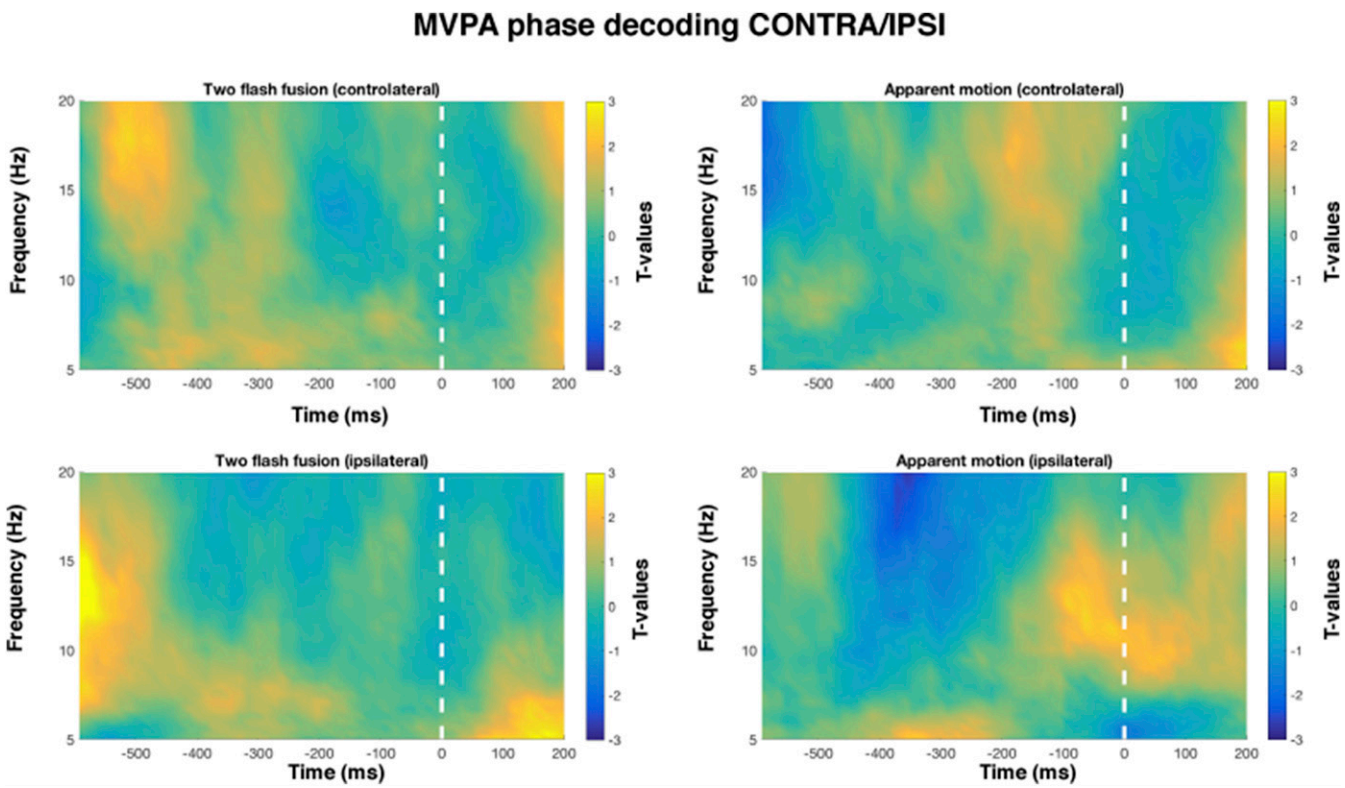

Fig. S2. Time/frequency plots showing phase-decoding accuracy obtained with a naive Bayes classifier searchlight [color-coded t values represent the group level difference against the chance level (i.e., 50% decoding accuracy)] as a function of the type of trial and the location of the electrodes relative to the stimulus hemifield (contralateral and ipsilateral). We performed this complementary analysis, which involved "mirroring" all channels for trials containing stimuli appearing on the right hemifield, to investigate whether there could be effects systematically occurring in the contralateral (or ipsilateral) side relative to the stimulus presentation. In this way, the effects that systematically occur contralaterally map on the right electrodes and the ipsilateral effects map on the left electrodes. However, no significant results emerged for the integration vs. segregation comparison (two-flash fusion trials: all corrected $P > 0.142$; apparent motion trials: all corrected $P > 0.099$). The cluster of channels plotted here for the contralateral plots is the same as in Fig. 3 (and is homologous in the left hemisphere for the ipsilateral plots). CONTRA/IPSI, controlateral/ipsilateral; MVPA, multivariate pattern analysis.

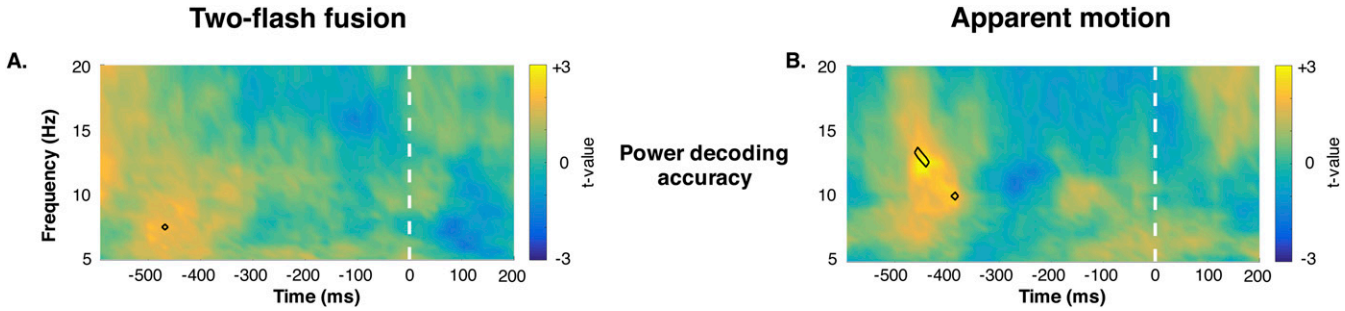

Fig. S3. Time/frequency plots showing power-decoding accuracy obtained with a naive Bayes classifier searchlight [color-coded t values represent the group level difference against the chance level (i.e., 50% decoding accuracy)] as a function of the type of trial [(*A*) two-flash fusion trials; (*B*) apparent motion trials]. The outlined areas of the plots delimit the intersection of time/frequency points where a significant difference was obtained with cluster-corrected permutation tests in the four right parieto-occipital channels with highest decoding accuracy resulted from the phase-decoding analysis.